Evaluation of Thermal Deformation in Electronic Packages

Hyeon Gyu Beom,* Kyoung Moon Jeong
Department of Mechanical Engineering, Chonnam National University

Thermal deformation in an electronic package due to thermal strain mismatch is investigated. The warpage and the in-plane deformation of the package after encapsulation is analyzed using the laminated plate theory. An exact solution for the thermal deformation of an electronic package with circular shape is derived. Theoretical results are presented on the effects of the layer geometries and material properties on the thermal deformation. Several applications of the exact solution to electronic packaging product development are illustrated. The applications include lead on chip package, encapsulated chip on board and chip on substrate.

Key Words : Thermal Deformation, Electronic Package, Warpage, Laminated Plate Theory, Analytic Solution

1. Introduction

Thermal deformation of a plastic package after encapsulation is a potential reliability concern (Lau, 1993). After encapsulation, thermal deformation is created within a package due to thermal expansion mismatch between the constituent materials as it cools from the molding temperature to room temperature. Warpage of the molded package becomes more serious as the package size increases and the package thickness decreases. The package warpage can cause problems with mounting the package onto a printed circuit board and often results in premature solder joint failures. In-plane deformation of the package caused by thermal loading is also a major cause of solder reliability problems.

Studies on warpage of plastic packages have been performed recently. Suhir and Manzione (1992) developed an analytical stress model for the evaluation of thermally induced bow of a large plastic package due to the nonuniform distribution of temperature in the through-thickness direction after a molding cycle. They treated a plastic package as a rectangular homogeneous plate. Subsequently, Suhir (1993) obtained the analytic solution for warpage of thin plastic packages subjected to a uniform temperature change. In his work, a thin plastic package is treated as a composite plate under plane strain. Kelly *et al.* (1994, 1996) and Zheng *et al.* (1997) employed the finite element techniques to predict warpage in plastic quad flat packs after encapsulation. Complicated geometry of the electronic packages makes it difficult to obtain the analytic solutions for displacement distributions in real packages. A closed form solution for thermal deformation of plastic package has not yet been derived.

The purpose of this study is to provide a method for evaluation of thermal deformation in an electronic package, due to thermal strain mismatch. A thin plastic package can be treated as a composite plate manufactured at an elevated temperature and subsequently cooled down to the room temperature. The problem of plate bending of the multilayered structure subjected small deformation is approached using the classical plate theory. An exact solution for the thermal deformation of an electronic package with a

* Corresponding Author,
E-mail : hgbeom@chonnam.ac.kr
TEL : +82-62-530-1682 ; **FAX** : +82-62-530-1689
Department of Mechanical Engineering, College of Engineering, Chonnam National University, 300 Yongbong-dong, Kwangju, 500-757 Korea. (Manuscript **Received** August 23, 1999 ; **Revised** November 16, 1999)

circular shape is derived in this paper. Theoretical results are presented on the effects of the layer geometries and material properties on the thermal deformation. Several applications of the exact solution to electronic packaging product development are illustrated. The applications include lead on chip package, encapsulated chip on board and chip on substrate.

2. Formulation

A thin plastic package can be treated as a composite plate manufactured at an elevated temperature and subsequently cooled down to the room temperature. Consider a deformation of a plate composed of thin layers of isotropic linear elastic material. The cross section of the plate is shown schematically in Fig. 1. The plate has constant thickness h. A temperature change ΔT from the initial stress-free state are uniform in the plate. The temperature change is assumed to be the same throughout the laminate. According to the classical laminated plate theory, the displacements at any point of a plate are written as (Jones, 1975)

$$u_i=u_i^0-x_3w_{,i}(x_1, x_2),\ (i=1, 2),\qquad (1)$$
$$u_3=w(x_1, x_2),$$

where u_i and u_3 are the in-plane and transverse displacements, respectively, u_i^0 is the in-plane displacement on the main plane, and the subscript comma(,) denotes a partial derivative with respective to the in-plane Cartesian coordinates, x_1 and x_2. The constitutive relations for the laminated plate have the following form:

$$N_{ij}=A_{12}(\varepsilon_{kk}^0-2\varepsilon^{0T})\delta_{ij}+(A_{11}-A_{12})(\varepsilon_{ij}^0-\varepsilon^{0T}\delta_{ij})+B_{12}\chi_{kk}\delta_{ij}+(B_{11}-B_{12})\chi_{ij},$$
$$M_{ij}=B_{12}\varepsilon_{kk}^0\delta_{ij}+(B_{11}-B_{12})\varepsilon_{ij}^0+D_{12}(\chi_{kk}-2\chi^T)\delta_{ij}+(D_{11}-D_{12})(\chi_{ij}-\chi^T\delta_{ij}).\qquad (2)$$

Here N_{ij} and M_{ij} are the resultant stress and moment defined as $N_{ij}=\int_{-h^0}^{h-h^0}\sigma_{ij}dx_3$ and $M_{ij}=\int_{-h^0}^{h-h^0}x_3\sigma_{ij}dx_3$, respectively, where σ_{ij} is the stress. ε_{ij}^0 and χ_{ij} are the main plane strain and the curvature defined as $\varepsilon_{ij}^0=\frac{1}{2}(u_{i,j}^0+u_{j,i}^0)$ and $\chi_{ij}=-w_{,ij}$, respectively. δ_{ij} is the Kronecker delta. A_{ij}, B_{ij} and D_{ij} are the extensional, coupling and bending stiffnesses, respectively, given as

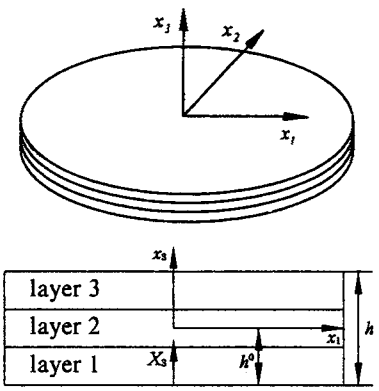

Fig. 1 Geometry of a multilayered plate

$$A_{ij}=\int_{-h^0}^{h-h^0}C_{ij}dx_3,\ B_{ij}=\int_{-h^0}^{h-h^0}x_3C_{ij}dx_3,$$
$$D_{ij}=\int_{-h^0}^{h-h^0}x_3^2C_{ij}dx_3,\ (ij=11, 12),\qquad (3)$$

where C_{11} and C_{12} are the stiffnesses given in terms of Young's modulus E and Poisson's ratio ν of the layer as $C_{11}=E/(1-\nu^2)$ and $C_{12}=\nu E/(1-\nu^2)$. ε^{0T} and χ^T are the thermal strain and the thermal curvature, respectively, given as

$$\varepsilon^{0T}=\frac{1}{\hat{A}}\int_{-h^0}^{h-h^0}\hat{C}\alpha\Delta Tdx_3,$$
$$\chi^T=\frac{1}{\hat{D}}\int_{-h^0}^{h-h^0}\hat{C}\alpha\Delta Tx_3dx_3,\qquad (4)$$

where $\hat{C}=C_{11}+C_{12}$, $\hat{A}=A_{11}+A_{12}$, $\hat{D}=D_{11}+D_{12}$ and α is the coefficient of thermal expansion. In this paper, the repetition of an index in a term denotes a summation with respect to that index over its range 1 to 2 for a Roman letter lowercase, unless indicated otherwise. Without loss of generality, we can place the main plane ($x_3=0$) at the distance

$$h^0=\int_0^h X_3C_{11}dX_3/\int_0^h C_{11}dX_3,\qquad (5)$$

from the lower surface of the plate. Here, $X_3(=x_3+h^0)$ is the vertical coordinate of the given point from the lowest surface of the plate. Clearly, (5) is equivalent to the condition $B_{11}=\int_{-h^0}^{h-h^0}x_3C_{11}dx_3=0$.

3. Analytic Solution

Many techniques and methods have been developed to evaluate the thermal deformation in electronic packages. Because of complicated geometry and highly nonlinear properties of the materials composing the packages, it is difficult to obtain the analytic solution for deformation distribution in real packages. To simplify the complexities, the following assumptions are made in this paper. The package is stress free and undeformed at the molding temperature. Mechanical properties of materials are linear elastic and independent of temperature. Perfect adhesion exists at the material interfaces within the package. The laminated plate theory is employed to analyze the warpage and the in-plane deformation of the package after encapsulation.

Consider thermal deformation of a circular laminate with radius R as shown in Fig. 2. The circular plate has the stiffness tensors A_{ij}, B_{ij} and D_{ij} $(ij=11, 12)$, and the stiffness tensors of the circular inhomogeneity with radius a are A^*_{ij}, B^*_{ij} and D^*_{ij}. We introduce cylindrical coordinates (r, θ, x_3) for convenience, and take the origin of coordinates at the center of the plate and denote by r the radial distance of the point in the main plane of the plate. All field quantities are independent of θ and are function of r alone. The main plane thermal strain and the thermal curvature prescribed in the laminate are : $\varepsilon^{0T}_{ij}=\varepsilon^{0T}\delta_{ij}$, $\kappa^T_{ij}=\kappa^T\delta_{ij}$ for $r>a$ and $\varepsilon^{0T*}_{ij}=\varepsilon^{0T*}\delta_{ij}$, $\kappa^{T*}_{ij}=\kappa^{T*}\delta_{ij}$ for $r<a$, respectively. The boundary conditions along the outer boundary of the plate at $r=R$ are:

$$t^0_i=0 \ \text{at} \ r=R, \qquad (6)$$
$$V_r=0, \ M_{rr}=0 \ \text{at} \ r=R.$$

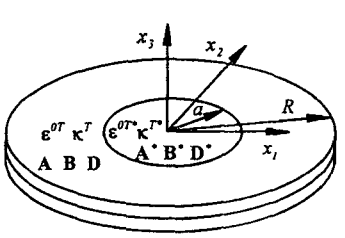

Fig. 2 Circular laminate with an inhomogeneity

Here t^0_i is the resultant in-plane traction given as $t^0_i=N_{ij}n_j$, where n_j is the unit vector normal to the plate edge and V_r is the Kirchhoff force. Applying the superposition principle, we can obtain solutions of the plate from the sum of solutions for problems a and b as shown in Fig. 3. The displacements for the plate are written as

$$u^0_i=u^{0(a)}_i+u^{0(b)}_i, \qquad (7)$$
$$w=w^{(a)}+w^{(b)},$$

where superscripts a and b in parentheses indicate the quantities associated with the problems a and b, respectively. For the problem a, the circular plate has the stiffness tensors A_{ij}, B_{ij} and D_{ij} $(ij=11, 12)$. The main plane thermal strain and the thermal curvature prescribed in the laminate are : $\varepsilon^{0T}_{ij}=\varepsilon^{0T}\delta_{ij}$, $\kappa^T_{ij}=\kappa^T\delta_{ij}$ throughout the plate, respectively. The boundary conditions for the problem a are :

$$t^{0(a)}_i=0 \ \text{at} \ r=R, \qquad (8)$$
$$V^{(a)}_r=0, \ M^{(a)}_{rr}=0 \ \text{at} \ r=R.$$

The problem a for the plate subjected to the boundary conditions (8) can be solved by taking $N^{(a)}_{ij}=0$ and $M^{(a)}_{ij}=0$ throughout the plate, which satisfies the in-plane boundary condition (8) as well as the equilibrium equation. Inversion of (2) for $N^{(a)}_{ij}=0$ and $M^{(a)}_{ij}=0$ gives the main plane strain and the curvature

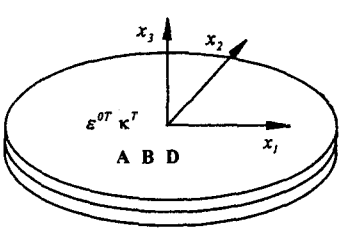

(a) Homogeneous circular plate

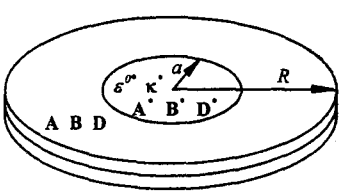

(b) Circular plate containing an inclusion with an equivalent eigenstrain

Fig. 3 Superposition of elastic fields in a circular plate

$$\varepsilon_{ij}^{0(a)}=\varepsilon^{0(a)}\delta_{ij}, \qquad (9)$$
$$\chi_{ij}^{(a)}=\chi^{(a)}\delta_{ij}.$$

Here

$$\varepsilon^{0(a)}=(\hat{A}-\hat{B}\hat{D}^{-1}\hat{B})^{-1}(\hat{A}\varepsilon^{0T}-\hat{B}\chi^{T}), \qquad (10)$$
$$\chi^{(a)}=(\hat{D}-\hat{B}\hat{A}^{-1}\hat{B})^{-1}(\hat{D}\chi^{T}-\hat{B}\varepsilon^{0T}),$$

where $\hat{A}=A_{11}+A_{12}$, $\hat{B}=B_{11}+B_{12}$ and $\hat{D}=D_{11}+D_{12}$. Integrating the strain-displacement relationships, the closed form of the corresponding displacement can be expressed as

$$u_r^{0(a)}=\varepsilon^{(a)}r,$$
$$u_\theta^{0(a)}=0, \qquad (11)$$
$$w^{(a)}=-\frac{1}{2}\chi^{(a)}r^2,$$

Next, consider problem b for a circular finite plate with a radius R as shown in Fig. 3. The circular plate has the stiffnesses A_{ij}, B_{ij} and D_{ij}, and the stiffnesses of the circular inhomogeneity with a radius a are A_{ij}^*, B_{ij}^* and D_{ij}^*. The main plane eigenstrain ε_{ij}^{0*} and the eigencurvature χ_{ij}^* prescribed in the circular inhomogeneity are determined so as to satisfy the condition for the equivalency of the resultant stress and moment in the circular inhomogeneity. Making use of (2), (7) and (11), it can be shown that

$$\varepsilon_{ij}^{0*}=\varepsilon^{0*}\delta_{ij} \qquad (12)$$
$$\chi_{ij}^{*}=\chi^{*}\delta_{ij}.$$

where $\varepsilon^{0*}=\varepsilon^{0T*}-\varepsilon^{0(a)}-\hat{A}^{*-1}\hat{B}^{*}\chi^{(a)}$ and $\chi^{*}=\chi^{T*}-\chi^{(a)}-\hat{D}^{*-1}\hat{B}^{*}\varepsilon^{0(a)}$. The boundary conditions for the problem b are :

$$t_i^{0(b)}=0 \ at \ r=R, \qquad (13)$$
$$V_r^{(b)}=0,\ M_{rr}^{(b)}=0 \ at \ r=R.$$

Recently, Beom and Earmme (1999) have obtained the closed form solution for the displacements for the problem b by using the equivalent eigenstrain method. The closed form solution for the displacement fields is written as

$$u_r^{0(b)}=\left\{\frac{1+v^A}{2}+p_{11}\right\}\varepsilon^{0**}r+p_{12}\chi^{**}r,\ u_\theta^{0(b)}=0,$$
$$w^{(b)}=-\frac{1}{2}\left[p_{21}\varepsilon^{0**}r^2+\left\{\frac{1}{2}(1+v^D)+p_{22}\right\}\chi^{**}r^2\right]$$
for $r<a$
$$u_r^{0(b)}=\left\{\frac{1+v^A}{2}\frac{a^2}{r}+p_{11}r\right\}\varepsilon^{0**}+p_{12}\chi^{**}r,$$
$$u_\theta^{0(b)}=0,$$
$$w^{(b)}=-\frac{1}{2}\left[p_{21}\varepsilon^{0**}r^2+\left\{\frac{1}{2}(1+v^D)\,a^2(2\ln r/a+1)+p_{22}r^2\right\}\chi^{**}\right] \text{ for } r>a. \qquad (14)$$

Here $v^A=A_{12}/A_{11}$, $v^D=D_{12}/D_{11}$ and the constants p_{ij} are presented in Appendix A. ε^{0**} and χ^{**} are the equivalent eigenstrain and the equivalent eigencurvature for the circular plate, which are written in terms of ε^{0*} and χ^{*} as follows

$$\begin{Bmatrix}\varepsilon^{0**}\\ \chi^{**}\end{Bmatrix}=\begin{bmatrix}F_{11} & F_{12}\\ F_{21} & F_{22}\end{bmatrix}\begin{Bmatrix}\varepsilon^{0*}\\ \chi^{*}\end{Bmatrix}, \qquad (15)$$

where F_{ij} are presented in Appendix A. Since the solutions of the displacements for problems a and b are determined as above, the complete solutions for the displacement field for the circular plate are written from (11) and (14) as

$$u_r^0(r)=\left\{\frac{1+v^A}{2}+p_{11}\right\}\varepsilon^{0**}r+(\varepsilon^{(a)}+p_{12}\chi^{**})\,r,$$
$$u_\theta^0(r)=0,$$
$$w(r)=-\frac{1}{2}\left[(\chi^{(a)}+p_{21}\varepsilon^{0**})\,r^2+\left\{\frac{1}{2}(1+v^D)+p_{22}\right\}\chi^{**}r^2\right] \text{ for } r<a$$
$$u_r^0(r)=\left\{\frac{1+v^A}{2}\frac{a^2}{r}+p_{11}r\right\}\varepsilon^{0**}+(\varepsilon^{(a)}+p_{12}\chi^{**})\,r,\ u_\theta^0(r)=0,$$
$$w(r)=-\frac{1}{2}\left[(\chi^{(a)}+p_{21}\varepsilon^{0**})\,r^2+\left\{\frac{1}{2}(1+v^D)\,a^2(2\ln r/a+1)+p_{22}r^2\right\}\chi^{**}\right] \text{ for } r>a. \qquad (16)$$

Thus, the in-plane displacement at any point of a plate is obtained from (1) and (16) as

$$u_r(r,x_3)=\left[\left\{\frac{1+v^A}{2}+p_{11}\right\}\varepsilon^{0**}+\varepsilon^{(a)}+p_{12}\chi^{**}\right]r+x_3\left[\chi^{(a)}+p_{21}\varepsilon^{0**}+\left\{\frac{1}{2}(1+v^D)+p_{22}\right\}\chi^{**}\right]r$$
for $r<a$,
$$u_r(r,x_3)=\left\{\frac{1+v^A}{2}\frac{a^2}{r}+p_{11}r\right\}\varepsilon^{0**}+(\varepsilon^{(a)}+p_{12}\chi^{**})\,r+x_3\left[(\chi^{(a)}+p_{21}\varepsilon^{0**})\,r+\left\{\frac{1}{2}(1+v^D)\frac{a^2}{r}+p_{22}r\right\}\chi^{**}\right] \text{ for } r>a. \qquad (17)$$

The analytic solution (17) shows dependence of the thermal deformation on the layer geometries and material properties. Similarly, the corre-

sponding resultant stress and moment can be evaluated from (2) and (16) (Appendix B). It is noted that the approach via the through-thickness averaging approach in the lamination theory has a limitation, i. e. it can not determine the local stress fields which appear at the three junctions between the individual layers and the elastic inhomogeneity. However, the solution of the resultant stress and moment obtained in this paper provides an overview of the problem and the locations of the critical elements in the structure.

4. Deformation of Electronic Packages

This section illustrates several applications of the exact solution obtained in the previous section to electronic packages. The applications include lead on chip package, encapsulated chip on board and chip on substrate as shown in Fig. 4. The technique developed for prediction of the thermal deformation in a thin electronic package is applicable to optimal design of a package with sufficiently small warpage and in-plane deformation.

Consider thermal deformation of a lead on chip package as shown in Fig. 4(a). A thin small outline package (TSOP) is a typical example of the lead on chip package. The circular chip with radius a and thickness h^{chip} is embedded in a triple layered plate with thickness h. The thicknesses of three layers composing the laminate are $h^{(1)}$, $h^{(2)}$ and $h^{(3)}$, respectively. The distance from the lowest surface of the plate to the main plane h^0, the stiffness tensors of the triple layered plate A_{ij}, B_{ij} and D_{ij}, and the stiffness tensors of the laminate containing the chip A^*_{ij}, B^*_{ij} and D^*_{ij} can be easily written in terms of $h^{(L)}$, $C^{(L)}_{ij}$ $(L=1, 2, 3)$, h^{chip} and C^{chip}_{ij} from the definitions in the section 2, which are presented in Appendix C. Here the superscripts 1, 2 and 3 in the parentheses represent the quantities associated with the layers 1, 2 and 3, respectively, and the superscript chip denotes the quantities associated with the silicon chip. The thermal strain and the thermal curvature prescribed in the laminate are : $\varepsilon^{0T}_{ij}=\varepsilon^{0T}\delta_{ij}$, $\chi^{T}_{ij}=\chi^{T}\delta_{ij}$ for $r>a$ and $\varepsilon^{0T*}_{ij}=\varepsilon^{0T*}\delta_{ij}$, $\chi^{T*}_{ij}=\chi^{T*}\delta_{ij}$ for $r<a$, respectively, where ε^{0T}, χ^{T}, ε^{0T*} and

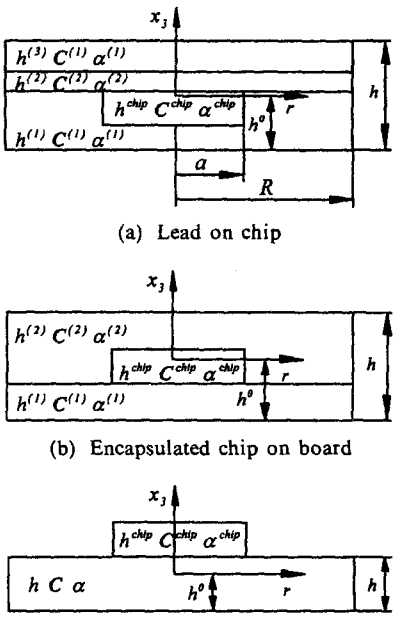

Fig. 4 Cross section of axisymmetric packages.

x^{T*} are presented in Appendix C. The material of layers 1 and 3 is molding compound and the layer 2 material is alloy 42. The material properties used in analysis of thermal deformation for the lead on chip package are listed in Table 1. For three specific values of $h^{(3)}/h$, the normalized radial displacement $\tilde{u}^m_r$ on the mid plane at $x_3=\frac{1}{2}h-h^0$ and the normalized transverse displacement $\tilde{w}$ are plotted as a function of r/R in Fig. 5. Here $\tilde{u}^m_r$ and $\tilde{w}$ are defined as $\tilde{u}^m_r(r)=\dfrac{u_r(r, \frac{1}{2}h-h^0)}{\alpha^{chip}\Delta TR}$ and $\tilde{w}(r)=\dfrac{w(r)}{\alpha^{chip}\Delta TR^2/h}$, respectively. The numerical values used in the computation are as follows : $h^{(1)}/h=0.875-h^{(3)}/h$, $h^{(2)}/h=0.125$, $h^{chip}/h=0.3$, $a/R=2/3$, $h=1$ mm and $R=15$mm. For the temperature change $\Delta T=150$°C, $\alpha^{chip}\Delta TR=6.75\mu$m and $\alpha^{chip}\Delta TR^2/h=101.25\mu$m. Figure 5 illustrates the effect of the layer geometries on in-plane deformation and warpage of the package. The thermal deformation of the lead on chip package is influenced by the location of the chip attached to the lead frame. Figure 5 shows that the influence of location of the chip on the in-plane deformation is quite

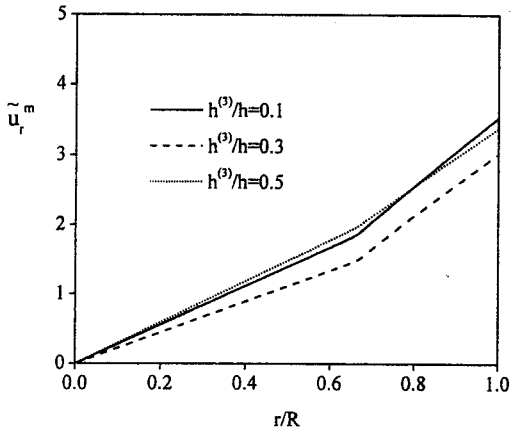

(a) Normalized radial displacement

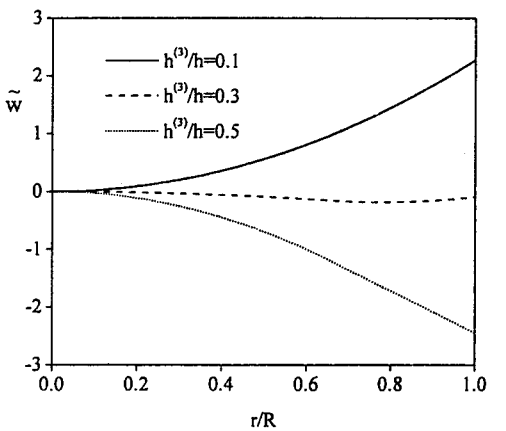

(b) Normalized transverse displacement

Fig. 5 Normalized displacements for lead on chip package as a function of r/R.

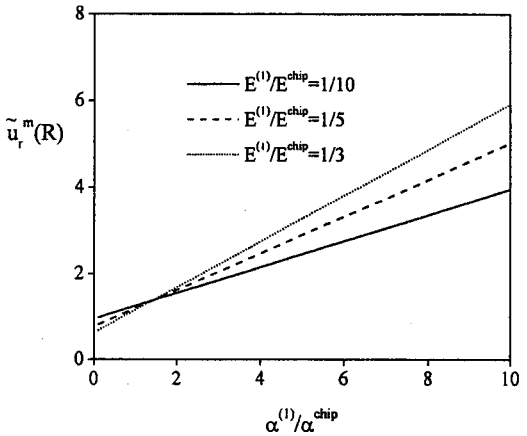

(a) Normalized radial displacement

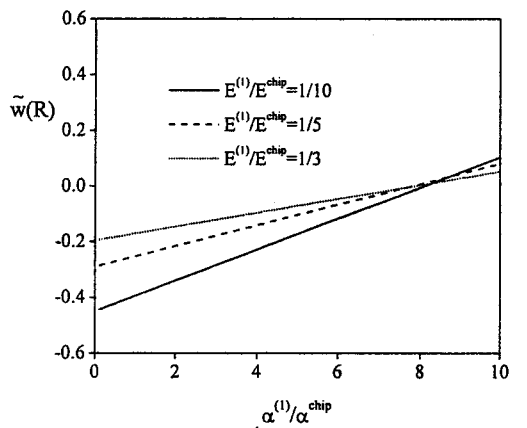

(b) Normalized transverse displacement

Fig. 6 Effect of material properties on thermal deformation of lead on chip package.

small. However, the influence is very strong for the warpage. Figure 6 shows the effects of the material properties of the molding compound on the thermal deformation. Here the numerical calculations are carried out for the package with $h^{(1)}/h=0.575$ and $h^{(3)}/h=0.3$. It is seen from Fig. 6 that the Young's modulus and coefficient of thermal expansion of the molding compound play in a significant role in the warpage as well as the in-plane deformation. Figures 5 and 6 show that the influence of the layer geometries and material properties on warpage and in-plane deformation of the packages is very strong for the large size package. The warpage sensitivity of different packages to changes in the layer geometries and material properties is higher as the thickness of the package decreases.

Next, we consider thermal deformation of an encapsulated chip on board as shown in Fig. 4 (b). A plastic ball grid array (PBGA) is a typical example of the encapsulated chip on board. Bismaleimide Triazine (BT) substrate is normally used for this PBGA. The silicon chip is directly attached to the BT substrate. The circular chip with radius a and thickness h^{chip} is embedded in a bilayered plate with thickness h. The thicknesses of two layers composing the laminate are $h^{(1)}$ and $h^{(2)}$, respectively. The thermal strain and the thermal curvature prescribed in the laminate are : $\varepsilon_{ij}^{0T}=\varepsilon^{0T}\delta_{ij}$, $\chi_{ij}^{T}=\chi^{T}\delta_{ij}$ for $r>a$ and $\varepsilon_{ij}^{0T*}=\varepsilon^{0T*}\delta_{ij}$, $\chi_{ij}^{T*}=\chi^{T*}\delta_{ij}$ for $r<a$, respectively, where ε^{0T}, χ^{T}, ε^{0T*} and χ^{T*} are presented in Appendix D.

Table 1 Material properties used in analysis of thermal deformation.

Material	E (GPa)	ν	α (ppm/℃)
Silicon	170	0.25	3
Alloy 42	148	0.30	5
Molding Compound	28	0.25	17
BT	20	0.20	15

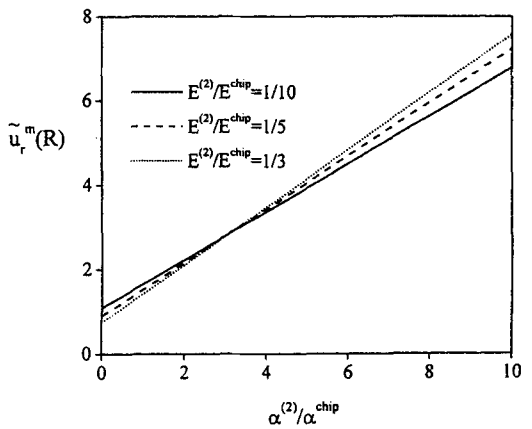

(a) Normalized radial displacement

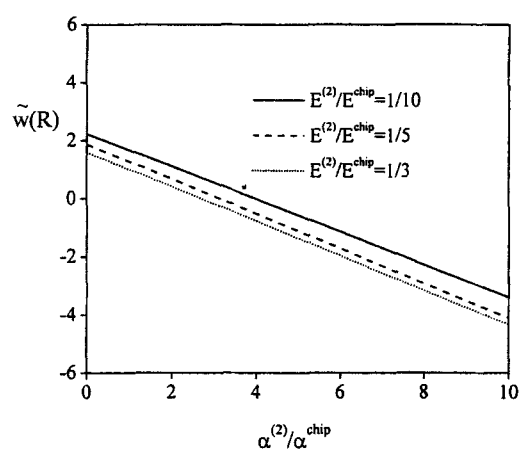

(b) Normalized transverse displacement

Fig. 7 Effect of material properties on thermal deformation of encapsulated chip on board.

The distance from the lowest surface of the plate to the main plane, h^0, and the stiffness tensors A_{ij}, B_{ij}, D_{ij}, A_{ij}^*, B_{ij}^* and D_{ij}^* can be easily written in terms of $h^{(L)}$, $C_{ij}^{(L)}$ $(L=1, 2)$, h^{chip} and C_{ij}^{chip},

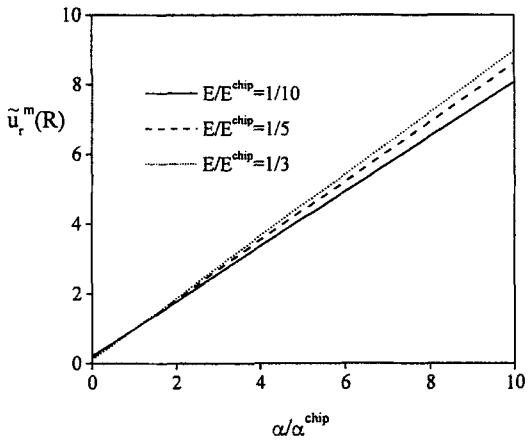

(a) Normalized radial displacement

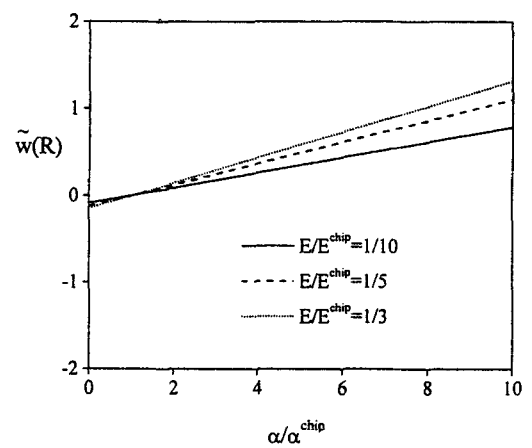

(b) Normalized transverse displacement

Fig. 8 Effect of material properties on thermal deformation of chip on substrate.

which are presented in Appendix D. The materials of layers 1 and 2 are BT substrate and molding compound, respectively. The material properties used in analysis of thermal deformation are listed in Table 1. Figure 7 illustrates the effect of the material properties of the molding compound on in-plane deformation and warpage of the package. Here the numerical calculations are carried out for the package with $h^{(1)}=0.3mm$, $h^{(2)}=1mm$, $h^{chip}=0.5mm$, $a=10mm$ and $R=20mm$.

Next, consider thermal deformation of a chip on board as shown in Fig. 4(c). The circular chip with radius a and thickness h^{chip} is attached in a plate with thickness h. The thermal strain and the

thermal curvature prescribed in the laminate are : $\varepsilon_{ij}^{0T}=\varepsilon^{0T}\delta_{ij}$, $\kappa_{ij}^{T}=\kappa^{T}\delta_{ij}$ for $r>a$ and $\varepsilon_{ij}^{0T*}=\varepsilon^{0T*}\delta_{ij}$, $\kappa_{ij}^{T*}=\kappa^{T*}\delta_{ij}$ for $r<a$, respectively, where ε^{0T}, κ^{T}, ε^{0T*} and κ^{T*} are presented in Appendix D. The distance from the lowest surface of the plate to the main plane, h^0, and the stiffness tensors A_{ij}, B_{ij}, D_{ij}, A_{ij}^*, B_{ij}^* and D_{ij}^* can be easily written in terms of h, C_{ij}, h^{chip} and C_{ij}^{chip}, which are presented in Appendix D. The material of the substrate is BT. Figure 8 illustrates the effect of the material properties of the substrate on in-plane deformation and warpage of the package. Here the numerical calculations are carried out for the package with $h=0.3mm$, $h^{chip}=0.5mm$, $a=10mm$ and $R=20mm$.

5. Conclusions

Thermal deformation in an electronic package due to thermal strain mismatch is investigated. The warpage and the in-plane deformation of the package after encapsulation is analyzed using the laminated plate theory. An exact solution for thermal deformation of an electronic package with a circular shape is derived. Theoretical results are presented on the effects of the layer geometries and material properties on the thermal deformation. Several applications of the exact solution to electronic packaging product development are illustrated. The applications include lead on chip package, encapsulated chip on board and chip on substrate. The layer geometries and material properties composing the packages play in a significant role in the warpage and in-plane deformation of the packages. It is shown that the influence of the layer geometries and material properties on warpage and in-plane deformation of the packages is very strong for the large size packages. The warpage sensitivity of different packages to changes in the layer geometries and material properties is higher as the thickness of the package decreases.

Acknowledgment

This study was financially supported by Chonnam National University in the program, 1998.

References

Beom, H. G. and Earmme, Y. Y., 1999, "The Elastic Field of an Elliptic Cylindrical Inclusion in a Laminate with Multiple Isotropic Layers," *ASME Journal of Applied Mechanics*, Vol. 66, pp. 165~171.

Jones, R. M., 1975, *Mechanics of Composite Materials*, McGraw-Hill, New York.

Kelly, G., Lyden, C., Lawton, W., Barrett, J., Saboui, A., Exposito, J. and Lamourelle, F., 1994, "Accurate Predictions of PQFP Warpage," *Proceedings of the 44th Electronic Components and Technology Conference*, pp. 102~106.

Kelly, G., Lyden, C., Lawton, W., Barrett, J., Saboui, A., Pape, H. and Peters, H. J. B., 1996, "Importance of Molding Compound Chemical Shrinkage in the Stress and Warpage Analysis of PQFP's," *IEEE Transactions on Components, Packaging, and Manufacturing Technology Part B*, Vol. 19, pp. 296~300.

Lau, J. H., 1993, *Thermal Stress and Strain in Microelectronics Packaging*, Van Nostrand Reinhold, New York.

Suhir, E., 1993, "Predicted Bow of Plastic Packages of Integrated Circuit (IC) Devices," *J. Reinforced Plastics & Composites*, Vol. 12, pp. 952~972.

Suhir, E. and Manzione, L. T., 1992, "Predicted Bow of Plastic Packages Due to the Nonuniform Through-Thickness Distribution of Temperature," *ASME Journal of Electronic Packaging*, Vol. 114, pp. 329~335.

Zheng, D., Hwang, R. P., Dou, X., Yeh, C., Prakash, M., Boardman, K. and Ridsdale, G., 1997, "Warpage Analysis of 144-Pin TQFP During Reflow Using Image Processing," *Proceedings of the 47th Electronic Components and Technology Conference*, Vol. 2, pp. 1176~1181.

Appendix A

The constants p_{ij} are:

$$p_{11}=\frac{1+v^A}{2J}\frac{a^2}{R^2}[\bar{D}A(1-v^A)+B^2],$$

$$p_{12}=-\frac{1+v^D}{2J}\frac{a^2}{R^2}[\hat{D}+D(1-v^D)]B,$$

$$p_{21}=-\frac{1+v^A}{2J}\frac{a^2}{R^2}[A(1-v^A)+\hat{A}]B,$$

$$p_{22}=\frac{1+v^D}{2J}\frac{a^2}{R^2}[B^2+\hat{A}D(1-v^D)], \quad \text{(A1)}$$

where $A=A_{11}$, $B=B_{12}$, $D=D_{11}$ and $J=\hat{A}\hat{D}-B^2$. The matrix $\boldsymbol{F}$ is given by $\boldsymbol{F}=\boldsymbol{L}^{-1}$, where the components of L_{ij} are

$$L_{11}=\frac{1}{\hat{A}^*}\{(\hat{A}^*-\hat{A})q_{11}+(\hat{B}^*-\hat{B})q_{21}+\hat{A}\},$$

$$L_{12}=\frac{1}{\hat{A}^*}\{(\hat{A}^*-\hat{A})q_{12}+(\hat{B}^*-\hat{B})q_{22}\},$$

$$L_{21}=\frac{1}{\hat{D}^*}\{(\hat{B}^*-\hat{B})q_{11}+(\hat{D}^*-\hat{D})q_{21}\},$$

$$L_{22}=\frac{1}{\hat{D}^*}\{(\hat{B}^*-\hat{B})q_{12}+(\hat{D}^*-\hat{D})q_{22}+\hat{D}\}, \quad \text{(A2)}$$

where $q_{11}=p_{11}+\frac{1+v^A}{2}$, $q_{12}=p_{12}$, $q_{21}=p_{21}$ and $q_{22}=p_{22}+\frac{1+v^D}{2}$.

Appendix B

$$N_{rr}=N_{\theta\theta}=A(1+v^A)\left[\left\{p_{11}-\frac{1}{2}(1-v^A)\right\}\varepsilon^{0**}+p_{12}\chi^{**}\right]+B\left[p_{21}\varepsilon^{0**}+\left\{p_{22}+\frac{1}{2}(1+v^D)\right\}\chi^{**}\right],$$

$$M_{rr}=M_{\theta\theta}=D(1+v^D)\left[\left\{p_{22}-\frac{1}{2}(1-v^D)\right\}\chi^{**}+p_{21}\varepsilon^{0**}\right]+B\left[p_{12}\chi^{**}+\left\{p_{11}+\frac{1}{2}(1+v^A)\right\}\varepsilon^{0**}\right],$$

$N_{r\theta}=M_{r\theta}=0$ for $r<a$, (B1)

$$N_{rr}=A(1+v^A)\left[\left\{p_{11}-\frac{1}{2}(1-v^A)\frac{a^2}{r^2}\right\}\varepsilon^{0**}+p_{12}\chi^{**}\right]+B\left[p_{21}\varepsilon^{0**}+\left\{p_{22}+\frac{1}{2}(1+v^D)\frac{a^2}{r^2}\right\}\chi^{**}\right],$$

$$N_{\theta\theta}=A(1+v^A)\left[\left\{p_{11}+\frac{1}{2}(1-v^A)\frac{a^2}{r^2}\right\}\varepsilon^{0**}+p_{12}\chi^{**}\right]+B\left[p_{21}\varepsilon^{0**}+\left\{p_{22}-\frac{1}{2}(1+v^D)\frac{a^2}{r^2}\right\}\chi^{**}\right],$$

$$M_{rr}=D(1+v^D)\left[\left\{p_{22}-\frac{1}{2}(1-v^D)\frac{a^2}{r^2}\right\}\chi^{**}+p_{21}\varepsilon^{0**}\right]+B\left[p_{12}\chi^{**}+\left\{p_{11}+\frac{1}{2}(1+v^A)\frac{a^2}{r^2}\right\}\varepsilon^{0**}\right],$$

$$M_{\theta\theta}=D(1+v^D)\left[\left\{p_{22}+\frac{1}{2}(1-v^D)\frac{a^2}{r^2}\right\}\chi^{**}+p_{21}\varepsilon^{0**}\right]+B\left[p_{12}\chi^{**}+\left\{p_{11}-\frac{1}{2}(1+v^A)\frac{a^2}{r^2}\right\}\varepsilon^{0**}\right],$$

$N_{r\theta}=M_{r\theta}=0$ for $r>a$,

where $A=A_{11}$, $B=B_{12}$ and $D=D_{11}$.

Appendix C

The distance from the lowest surface of the plate to the main plane for the lead on chip package is given by

$$h^0=\frac{1}{2}\frac{C_{11}^{(1)}\{h^{(1)2}+h^2-(h^{(1)}+h^{(2)})^2\}+C_{11}^{(2)}\{(h^{(1)}+h^{(2)})^2-h^{(1)2}\}}{C_{11}^{(1)}(h^{(1)}+h^{(3)})+C_{11}^{(2)}h^{(2)}}. \quad \text{(C1)}$$

The stiffness tensors are given by

$$\begin{aligned}
A_{ij}&=C_{ij}^{(1)}(h^{(1)}+h^{(3)})+C_{ij}^{(2)}h^{(2)},\\
B_{ij}&=\frac{1}{2}[C_{ij}^{(1)}\{(h^{(1)}-h^0)^2-h^{02}+(h-h^0)^2\\
&\quad-(h^{(1)}+h^{(2)}-h^0)^2\}\\
&\quad+C_{ij}^{(2)}\{(h^{(1)}+h^{(2)}-h^0)^2-(h^{(1)}-h^0)^2\}]\\
D_{ij}&=\frac{1}{3}[C_{ij}^{(1)}\{(h^{(1)}-h^0)^3-h^{03}+(h-h^0)^3\\
&\quad-(h^{(1)}+h^{(2)}-h^0)^3\}\\
&\quad+C_{ij}^{(2)}\{(h^{(1)}+h^{(2)}-h^0)^3-(h^{(1)}-h^0)^3\}]\\
A_{ij}^*&=C_{ij}^{(1)}(h^{(1)}-h^{chip}+h^{(3)})+C_{ij}^{chip}h^{chip}+C_{ij}^{(2)}h^{(2)},\\
B_{ij}^*&=\frac{1}{2}[C_{ij}^{(1)}\{(h^{(1)}-h^{chip}-h^0)^2-h^{02}+(h\\
&\quad-h^0)^2-(h^{(1)}+h^{(2)}-h^0)^2\}\\
&\quad+C_{ij}^{chip}\{(h^{(1)}-h^0)^2-(h^{(1)}-h^{chip}-h^0)^2\}\\
&\quad+C_{ij}^{(2)}\{(h^{(1)}+h^{(2)}-h^0)^2-(h^{(1)}-h^0)^2\}]\\
D_{ij}^*&=\frac{1}{3}[C_{ij}^{(1)}\{(h^{(1)}-h^{chip}-h^0)^3-h^{03}+(h\\
&\quad-h^0)^3-(h^{(1)}+h^{(2)}-h^0)^3\}\\
&\quad+C_{ij}^{chip}\{(h^{(1)}-h^0)^3-(h^{(1)}-h^{chip}-h^0)^3\}\\
&\quad+C_{ij}^{(2)}\{(h^{(1)}+h^{(2)}-h^0)^3-(h^{(1)}-h^0)^3\}].
\end{aligned} \quad \text{(C2)}$$

It is noted that B_{11}^* is not zero in general since h^0 is determined so as to satisfy $B_{11}=0$ only. The thermal strain and the thermal curvature are given by

$$\varepsilon^{0T}=\frac{\Delta T}{\hat{A}}[\hat{C}^{(1)}\alpha^{(1)}(h^{(1)}+h^{(3)})+\hat{C}^{(2)}\alpha^{(2)}h^{(2)}],$$

$$\chi^T=\frac{\Delta T}{2\hat{D}}[\hat{C}^{(1)}\alpha^{(1)}\{(h^{(1)}-h^0)^2-h^{02}+(h-h^0)^2-(h^{(1)}+h^{(2)}-h^0)^2\}$$

$$+\hat{C}^{(2)}\alpha^{(2)}\{(h^{(1)}+h^{(2)}-h^0)^2-(h^{(1)}-h^0)^2\}].$$

$$\varepsilon^{0T*}=\frac{\Delta T}{\hat{A}^*}[\hat{C}^{(1)}\alpha^{(1)}(h^{(1)}-h^{chip}+h^{(3)})+\hat{C}^{chip}\alpha^{chip}h^{chip}+\hat{C}^{(2)}\alpha^{(2)}h^{(2)}],$$

$$x^{T*}=\frac{\Delta T}{2\hat{D}^*}[\hat{C}^{(1)}\alpha^{(1)}\{(h^{(1)}-h^{chip}-h^0)^2-h^{02}+(h-h^0)^2-(h^{(1)}+h^{(2)}-h^0)^2\}+\hat{C}^{chip}\alpha^{chip}\{(h^{(1)}-h^0)^2-(h^{(1)}-h^{chip}-h^0)^2\}+\hat{C}^{(2)}\alpha^{(2)}\{(h^{(1)}+h^{(2)}-h^0)^2-(h^{(1)}-h^0)^2\}]. \quad (C3)$$

Appendix D

For the encapsulated chip on board, it can be shown that

$$h^0=\frac{1}{2}\frac{C_{11}^{(1)}h^{(1)2}+C_{11}^{(2)}(h^2-h^{(1)2})}{C_{11}^{(1)}h^{(1)}+C_{11}^{(2)}h^{(2)}},$$

$$A_{ij}=C_{ij}^{(1)}h^{(1)}+C_{ij}^{(2)}h^{(2)},$$

$$B_{ij}=\frac{1}{2}[C_{ij}^{(1)}\{(h^{(1)}-h^0)^2-h^{02}\}+C_{ij}^{(2)}\{(h-h^0)^2-(h^{(1)}-h^0)^2\}],$$

$$D_{ij}=\frac{1}{3}[C_{ij}^{(1)}\{(h^{(1)}-h^0)^3-h^{03}\}+C_{ij}^{(2)}\{(h-h^0)^3-(h^{(1)}-h^0)^3\}],$$

$$\varepsilon^{0T}=\frac{\Delta T}{\hat{A}}(\hat{C}^{(1)}\alpha^{(1)}h^{(1)}+\hat{C}^{(2)}\alpha^{(2)}h^{(2)}),$$

$$x^T=\frac{\Delta T}{2\hat{D}}[\hat{C}^{(1)}\alpha^{(1)}\{(h^{(1)}-h^0)^2-h^{02}\}+\hat{C}^{(2)}\alpha^{(2)}\{(h-h^0)^2-(h^{(1)}-h^0)^2\}],$$

$$A_{ij}^*=C_{ij}^{(1)}h^{(1)}+C_{ij}^{chip}h^{chip}+C_{ij}^{(2)}(h^{(2)}-h^{chip}),$$

$$B_{ij}^*=\frac{1}{2}[C_{ij}^{(1)}\{(h^{(1)}-h^0)^2-h^{02}\}+C_{ij}^{chip}\{(h^{(1)}+h^{chip}-h^0)^2-(h^{(1)}-h^0)^2\}+C_{ij}^{(2)}\{(h-h^0)^2-(h^{(1)}+h^{chip}-h^0)^2\}],$$

$$D_{ij}^*=\frac{1}{3}[C_{ij}^{(1)}\{(h^{(1)}-h^0)^3+h^{03}\}+C_{ij}^{chip}\{(h^{(1)}+h^{chip}-h^0)^3-(h^{(1)}-h^0)^3\}+C_{ij}^{(2)}\{(h-h^0)^3-(h^{(1)}+h^{chip}-h^0)^3\}],$$

$$\varepsilon^{0T*}=\frac{\Delta T}{\hat{A}^*}[\hat{C}^{(1)}\alpha^{(1)}h^{(1)}+\hat{C}^{chip}\alpha^{chip}h^{chip}+\hat{C}^{(2)}\alpha^{(2)}(h^{(2)}-h^{chip})],$$

$$x^{T*}=\frac{\Delta T}{2\hat{D}^*}[\hat{C}^{(1)}\alpha^{(1)}\{(h^{(1)}-h^0)^2-h^{02}\}+\hat{C}^{chif}\alpha^{chip}\{(h^{(1)}+h^{chip}-h^0)^2-(h^{(1)}-h^0)^2\}+\hat{C}^{(2)}\alpha^{(2)}\{(h-h^0)^2-(h^{(1)}+h^{chip}-h^0)^2\}]. \quad (D1)$$

In the special case in which $h^{(1)}=h$, $C_{ij}^{(1)}=C_{ij}$, $\alpha^{(1)}=\alpha$, $h^{(2)}=0$, $C_{ij}^{(2)}=0$ and $\alpha^{(2)}=0$, (D1) is reduced to those for the chip on substrate shown in Fig. 4 (c).